

Application of diamond detectors to the dosimetry of 45 and 100 kVp therapy beams: comparison with a parallel-plate ionization chamber and Monte Carlo

Richard P Hugtenburg, Kristen Johnston, Graham J Chalmers and Alun H Beddoe

Imaging and Medical Physics Group, Queen Elizabeth Hospital, University Hospital Birmingham NHS Trust, Birmingham B15 2TH, UK

E-mail: richard.hugtenburg@university-b.wmids.nhs.uk

Received 19 March 2001, in final form 21 June 2001

Published 22 August 2001

Online at stacks.iop.org/PMB/46/2489

Abstract

Diamond detectors have become an increasingly popular dosimetric method where either high spatial resolution is required or where photon or electron spectra are likely to change with depth or field size. However, little work has been previously reported for superficial energies. This paper reports the response of a commercially available diamond detector (PTW Freiburg/IPTB Dubna) at 45 kVp (0.55 mm Al first HVL) and 100 kVp (2.3 mm Al first HVL) including dose and dose-rate linearity, percentage depth-dose and output factors as a function of applicator size. Comparisons are made with *Br. J. Radiol.* supplement 25 data, measurements using a PTW parallel-plate chamber and Monte Carlo simulations based on spectra determined from transmission measurements in aluminium. Excellent agreement was obtained for percentage depth-dose curves between Monte Carlo and diamond after correcting for sublinearity of the dose-rate response and energy dependence of the diamond detector. However, significant differences were noted between diamond/Monte Carlo and the parallel-plate chamber, which is attributed to the perturbation caused by the polyethylene base of the chamber

1. Introduction

Diamond detectors are in principle attractive for radiation measurements involving either small radiation fields where spatial resolution is important (Heydarian *et al* 1996) or in situations where changes in photon/electron spectra occur with depth or field size (Heydarian *et al* 1997). The near water equivalence of carbon ($Z = 6$ versus $Z = 7.4$ for soft tissue) ensures that mass stopping power and mass-energy absorption coefficient ratios of carbon to water, and therefore the radiation response, varies slowly over most of the therapeutic energy range. However, in the

superficial energy range considerable variations in the latter ratio occur because of the sensitivity of the photoelectric cross section to small variations in Z , so that the suitability of diamond as a practical detector in this region requires investigation. Diamond detectors have similar small dimensions to silicon diode detectors and exhibit high radiation dose sensitivity, low leakage current (Kozlov *et al* 1975) and a high resistance to radiation damage (Planskoy *et al* 1980).

While the dosimetric characteristics of commercially available diamond detectors have been reported for megavoltage electron beams (Heydarian *et al* 1993), as well as photon beams over a broad range of megavoltage energies (Heydarian *et al* 1997, Khrunov *et al* 1990, Rustgi 1995, Hoban *et al* 1994), there have been only two published reports to the authors' knowledge on the application of such detectors to measurement in the kilovoltage energy ranges (Planskoy 1980, Seuntjens *et al* 1999).

For a given bias voltage the charge current obtained from a diamond detector varies almost linearly with dose rate so that the detector can be considered to behave as a resistive element (Burgemeister 1981). However, recombination of charge does occur and the relationship between current, I , and dose rate, \dot{D} , is of the form $I \propto \dot{D}^\Delta$ (Fowler 1966), with the exponent Δ varying between 0.5 (for a pure crystal) and 1.0 for diamond crystals with a high level of impurities (where the equilibrium electron density in traps is very much greater than the density of free electrons); a large trap density results in short recombination times and therefore reduced sensitivity, so that there is always a trade-off between linearity and sensitivity. Nevertheless, by appropriate selection of diamond crystals of a suitable thickness and level of impurity it is possible to ensure that Δ approaches unity yet still maintain acceptable sensitivity.

This paper discusses the response of these detectors at two therapeutic x-ray tube potentials, 45 kVp and 100 kVp, including such characteristics as linearity with dose and dose rate, preirradiation requirements, percentage depth-dose (PDD) curves and the variation of output factors with applicator size.

A Monte Carlo model, based on a perfectly collimated point source with a spectrum that has been derived from transmission measurements through aluminium, enables computation of simple quality and mean-free path based corrections to the diamond detector measurements in water and the parallel-plate chamber in a water equivalent polyethylene based material. PDD and backscatter factors (BSF) have been computed for a range of circular applicators. Large cavity conditions and negligible perturbation to the photon fluence are assumed. These approximations are considered to be adequate in the circumstances. The method presented is practical and easily implemented as extensive information about the source and detector constructions is not required.

The experimental results are compared with data published in *Br. J. Radiol.* supplement 25 (BJR 1996) which gives BSF and PDD compiled as a function of first half-value-layer (HVL) and focus-to-surface distance (FSD) for a representative set of x-ray therapy beams. These data have been interpolated from our measurements of the first HVL of the two beams. This is not entirely satisfactory as a particular tube potential can have a range of first HVLs depending on the filtration.

2. Methods

2.1. The source

Measurements were conducted on a Philips RT-100 therapy unit, at 100 kVp (2.3 mm Al first HVL) and 45 kVp (0.55 mm Al first HVL). The tube has an anode angle of 45° , a nominal filtration of 1.2 mm Be and was used with in-house cylindrical applicators which project to field diameters of 5.08, 4.02, 3.08, 2.03 and 1.57 cm at 15 cm FSD.

2.2. The detectors and electrometer

A PTW-Freiburg/IPTP Dubna diamond detector (type 60003) was used in this work. It consists of a natural diamond plate with a thickness of 0.36 mm, a volume of 2.2 mm³ and an area of 6.1 mm². The crystal has a low concentration of nitrogen impurities and is embedded in a polystyrene cylinder which is fixed into a metallic stem. This arrangement is hermetically sealed in a plastic outer shell. The dark current is less than or equal to 5×10^{-12} A and the reference point of measurement is 1 mm below the detector surface at the centre of the sensitive area. A full description of the detector can be found in Heydarian *et al* (1993).

The parallel-plate chamber was a PTW (type 23342), 0.02 cm³ ionization chamber, (recommended in the 1996 IPEMB Code of Practice (Klevenhagen *et al* 1991)) which is claimed to have a very low energy dependence between 7.5 kV and 100 kV. It consists of a rectangular polyethylene block of length 61 mm, width 22 mm and height 14.4 mm containing a cylindrical sensitive measuring volume with diameter 5.2 mm and height 1 mm. The effective thickness of the entrance window is 2.5 mg cm⁻². The 1996 protocol offers no advice on the perturbation factor for this chamber which is assumed initially to be negligible. Results presented later in the paper and elsewhere (Ipe *et al* 2001, Perrin *et al* 2001) demonstrate that the magnitude and depth-dependent change of the perturbation factor are likely to be significant.

Ionization in the diamond detector and the parallel-plate chamber was measured with an NE Technology Farmer 2670 electrometer. Relative output factors were also measured in air using a 0.2 cm³ Farmer cylindrical ionization chamber (NE 2577).

2.3. The phantoms

Dose and dose-rate linearity for the diamond detector were measured in a QADOS MP1 mini water phantom; the dose measurement was in water and the dose-rate measurement used the empty phantom. All relative dose measurements with the parallel-plate chamber were conducted in solid phantoms. The PTW Freiburg RW1 solid water phantom used for PDD measurements is stated to be water equivalent to within $\pm 5.5\%$ in the range of 10–100 kV (Hermann *et al* 1985). It consists of 10 plates of varying thicknesses with dimensions of 13 cm \times 13 cm of total thickness 6.5 cm. An extra plate, 1.5 cm thick, was manufactured in-house and adapted to hold the parallel-plate chamber.

2.4. Dose linearity

The diamond detector was clamped in the arm attachment of the MP-1 tank and the relationship between the diamond detector output in a 5 cm diameter field and irradiation time was established for both beam qualities. Following a warming-up period of 20 min, the detector was preirradiated with a series of exposures each of 30 s duration (≈ 2.5 Gy) until the fluctuation between the readings was less than 1%. The measured dark current was subtracted from the subsequent measurements. The 'warm-up' protocol was applied for all the diamond detector measurements described below. The irradiation time of the diamond detector was increased successively up to a total absorbed dose of 8 Gy. A mean of three readings was taken for each exposure.

2.5. Dose-rate linearity

The diamond detector was clamped in the arm of the phantom which could be moved vertically using a mechanical thumbwheel attachment; a millimetre scale determined the position of

the detector. The dose rate to the detector was varied by changing its position over a 15 cm to 30 cm range from the source. The charge output in 30 s was determined at 1 cm step intervals within this range. A 0.2 cm³ Farmer ionization chamber was then substituted for the diamond detector in order to measure the relative dose at these points. This procedure was conducted for both beams with the 5 cm diameter applicator.

2.6. Depth-dose measurements

Depth doses for the diamond detector were measured in the MP1 water phantom. An exposure time of 30 s was chosen which corresponds to a surface dose of 2.5 Gy. The mean of three readings was taken at each depth. Depth-dose distributions were obtained for field sizes of 1.5 cm, 3 cm and 5 cm diameter for both beams. Corresponding depth-dose measurements for the parallel-plate chamber were obtained by varying the RW1 solid water phantom thickness while keeping the FSD constant.

2.7. Output factor measurements

The diamond detector was positioned face-up in the centre of the mini water tank filled with water to the detector surface to ensure full scatter conditions. The applicators were covered with polyester 'cling film' and aligned with the end just in contact with the water surface and measurements taken. The corresponding procedure was repeated for the parallel-plate chamber in the RW1 solid phantom. All measurements were normalized to the 5 cm diameter applicator.

Polyester sheets were also used to eliminate contaminant electrons for measurements with the parallel-plate chamber (Klevenhagen *et al* 1991). Ten and 70 μm sheets were used, which in combination with the 30 μm front face gives a thickness equivalent to the complete slowing down range of 40 and 80 keV electrons in a water equivalent material, comparable to typical electron contamination in the 45 and 100 kVp beams respectively. Electron contamination varies from 1.6% to 2.3% and 1.7% to 4.0% respectively with increased field size. The trend is in disagreement with that reported by Klevenhagen *et al* (1991), which may be due to the cylindrical applicator used; these have an increasing but evidently small scatter component from the side walls with increased field size.

2.8. Monte Carlo modelling of depth doses and backscatter

Primary incident spectra were derived for both the 45 and the 100 kVp beams from a simple transmission model (Waggener *et al* 1999) incorporating parametrization of mass attenuation and mass absorption coefficients as suggested by Ouellet and Schreiner (1991). Birch–Marshall spectra were used as a first approximation using the nominal peak voltage and filtration given by the manufacturer (Birch and Marshall 1979). The spectra were then tuned to agree with a set of transmission measurements through aluminium, to within the experimental uncertainty (rms of 1%) bound to within 10% (rms) of the original estimated spectrum, using a generalized gradient reduction technique.

The beam model assumes a point source collimated by apertures equivalent to the inner diameters of the cylindrical, open-ended lead applicators used in the clinical application. The Monte Carlo code EGS4 (Nelson *et al* 1985) was used for photon transport and bremsstrahlung creation down to 1 keV (PCUT and AP) and electron transport and secondary electron production down to 521 eV (ECUT and AE). Though normally a 10 keV lower bound is recommended for EGS4, various extensions improve the accuracy of simulation in the

superficial energy region, in particular the low-energy Compton scattering extension, LSCAT (Namito *et al* 1994). The simplified electron boundary crossing algorithm appropriate for low-energy electron transport, FIXTMX (Rogers 1984), was also used.

Our simplified modelling technique is supported by an examination of the contributions from the applicator walls. The contribution of scattered photons from the lead applicator walls is relatively small. Below the K-edge of lead (88 keV), scatter amounts to little more than 20% ($1 - \mu_{\text{en}}/\mu$) of the photon energy transfer. The applicators used and modelled in this paper are ideal for the purposes of validation; however, in general, the applicator walls can be a source of scatter, particularly if they are composed of lower- Z materials. These contributions will influence the shape of the PDD curves but they are not likely to greatly influence the energy response of the detector, suggesting that the simple modelling used in this paper is more generally applicable.

The scoring array consists of two concentric cylinders; the inner cylinder of diameter 6 mm is the scoring or sensitive region, which is larger than the sensitive area of the diamond detector but smaller than the area of the parallel-plate chamber. The outer cylinder is 200 mm in diameter. Both cylinders are sectioned into 0.1 mm slabs for the first 1 mm depth and into 1 mm slabs for depths up to 90 mm. The shallow slabs near the phantom surface are used to compute BSF. Primary radiation is labelled as such using LATCH so that electrons originating from primary photons are transported and scored until their cut-off energy is reached. Photon interactions are acknowledged in the routine AUSGAB by setting the IAUSFL variable to indicate whether a Compton, Rayleigh or photoelectric event has occurred.

The BSF has been defined, in a manner consistent with the influence of electron transport, at the depth of maximum dose (shown in Monte Carlo calculations to be between 100 and 200 μm for both beams). Particle splitting by a factor of 100 has been used for particles entering the sensitive volume for the first time. Extra weighting and labelling parameters were added to the stack and propagated accordingly by adjusting the two MORTRAN macro replacements in EGS4, COMIN/STACK and EXCHANGE-STACK.

2.9. Correction and normalization factors

Because photon spectra change with depth and applicator (field) size, corrections need to be made to the raw measurements for both the diamond and parallel plate detectors if any direct comparisons are to be made. On the reasonable assumption at superficial energies that all ion pairs detected are created by direct photon interaction with the carbon detector element, then the correction factor, $(D_{\text{water}}/D_{\text{carbon}})$, for any given quality, depth and field size is given by the ratio $(\overline{\mu_{\text{en}}/\rho})_{\text{water}}/(\overline{\mu_{\text{en}}/\rho})_{\text{carbon}}$, which are averages over the photon spectrum for the given depth and field size. This correction is in addition to the corrections for dose-rate nonlinearity. The situation is more complex for the parallel-plate chamber. Detection consists of measuring an electron fluence in air largely created in the entrance window and surrounding polyethylene. Assuming that the direct photon interaction with the air is negligible and that the electron spectrum is not significantly perturbed by the air cavity, then the dose in air must be converted first to dose in polyethylene and then to dose in the RW1 phantom material. The correction factor, for any given quality, depth and field size, is given by

$$\frac{D_{\text{RW1}}}{D_{\text{air}}} = \frac{\overline{S}_{\text{polyethylene}}}{\overline{S}_{\text{air}}} \cdot \frac{(\overline{\mu_{\text{en}}/\rho})_{\text{RW1}}}{(\overline{\mu_{\text{en}}/\rho})_{\text{polyethylene}}}. \quad (1)$$

In practice the stopping power ratio is slowly varying at these energies and can be neglected but can be calculated via equivalent manipulations of the electron spectra assuming that the electron spectra are relatively unperturbed.

The mass-energy absorption correction factors were readily computed using the above Monte Carlo procedures for all depths and field sizes used in this work.

An efficient means of calculating these corrections which avoids the storage of a spectrum for all depths and field sizes is to generate a Monte Carlo estimate as a summed series of the quantity from a single simulation in a water phantom, that is

$$\begin{aligned}
 D_X &= \int_{\varepsilon} \left(\frac{\mu_{\text{en}}}{\rho} \right)_X \frac{d\phi}{d\varepsilon} \varepsilon d\varepsilon \\
 &= \int_{\varepsilon} \left(\frac{\mu_{\text{en}}}{\rho} \right)_{\text{water}}^X \left(\frac{\mu_{\text{en}}}{\rho} \right)_{\text{water}} \frac{d\phi}{d\varepsilon} \varepsilon d\varepsilon \\
 &= \sum_i \left(\frac{\mu_{\text{en}}}{\rho} \right)_{\text{water}}^X \Delta\varepsilon_i / m
 \end{aligned} \tag{2}$$

where each Monte Carlo generated energy deposition, $\Delta\varepsilon_i$, a function of the energy of the contributing photon, ε , is weighted by the relatively slowly varying ratio of mass-energy absorption coefficients and m is the mass of the detector element.

In a similar fashion, an estimate of the changing mean-free path as a function of depth for the the RW1 material phantom can be computed by averaging photon step lengths as a function of depth and field size. A fictitious particle is generated for every photon interaction, which is transported in the RW1 material one step length before being deleted. An effective depth is computed by scaling according to the ratio of the mean-free path in water and the RW1 material. O'Connor's theorem (O'Connor 1957) is shown to be reasonably well preserved (to within 0.5% overall) with an effective density for RW1 of 0.989 for 100 kVp varying little with depth and field size and ranging from 0.985 to 0.990 with increasing depth and field size for 45 kVp where the photoelectric effect predominates.

3. Results

3.1. Backscatter factors

The relevant parameters for the two qualities measured are listed in table 1. BSF values for a 5 cm diameter, 15 cm FSD applicator including measured (via the PTW parallel-plate chamber and 0.2 cm³ Farmer chamber), Monte Carlo computed and the *Br. J. Radiol.* supplement 25 (BJR 1996) interpolated values are given. Also shown are the Monte Carlo computed ratio of energy responses of the diamond detector with depth to that of water for the same applicator. While the variation in response to field size is minimal at the surface and at all depths in the case of the 45 kVp beam, the relative response of the 100 kVp beam increases with depth to a maximum at 6 cm depth of 0.543 for the smallest (1.5 cm) applicator.

The measured BSF show reasonable agreement with the computation for both beams but lack precision due to uncertainties in the, as yet unestablished, perturbation factor for the parallel-plate chamber. Detailed Monte Carlo based modelling of the detector is planned to determine the magnitude and variation of this factor.

We have confidence in these new Monte Carlo results. Firstly, these calculations are based on a set of attenuation measurements in combination with theory and are hence matched more closely to the characteristics of the beam than interpolations based purely on the first HVL. Secondly, bound Compton scattering and Doppler broadening, which have not typically been incorporated in BSF calculations, increase the BSF by a small but detectable 0.7% for 45 kVp and 0.4% for 100 kVp. Thirdly, electron transport is often neglected in BSF calculations but has a small but detectable influence which would be expected to be larger at the higher of the

Table 1. Summary of the two energy modalities for the Philips RT-100 therapeutic superficial x-ray tube presented. BSF and the diamond detector response relative to water as a function of depth are given for an applicator of 5 cm diameter and 15 cm FSD. Uncertainties (in brackets, 2 sd) apply to the last significant figure.

(a) Tube and field characteristics		
	Peak voltage	
	45 kVp	100 kVp
Added filtration	0.55 mm Al	1.7 mm Al
First HVL	0.55 mm Al	2.3 mm Al
Meas. BSF	1.12(6)	1.17(6)
Monte Carlo	1.111(1)	1.211(2)
BJR suppl. 25	1.085	1.189
(b) Relative response diamond:water with depth (cm)		
Depth (cm)	45 kVp	100 kVp
0	0.402	0.469
0.1	0.402	0.473
0.2	0.402	0.475
0.5	0.402	0.479
1.0	0.403	0.485
1.5	0.404	0.491
2.0	0.406	0.496
2.5	0.407	0.500
3.0	0.408	0.505
3.5	0.409	0.509
4.0	0.410	0.513
5.0	0.412	0.519
6.0	0.414	0.526

two tube potentials. Enabling electron transport increases the BSF by 1.0% and 1.1% for the 45 and 100 kVp beams respectively.

3.2. Dose and dose-rate linearity

The variation of the integrated diamond detector output with dose was determined for both beams. The linear correlation coefficients were 0.9998 and 1.0000 respectively for doses ranging up to 8 Gy.

A least-squares calculation of the relation between the logarithm of dose rate and diamond detector current yielded Δ values of 0.970 ± 0.015 and 0.975 ± 0.003 for the 45 kVp and 100 kVp beams respectively.

3.3. Percentage depth dose

Percentage depth doses (PDD) are plotted in figure 1 for the 45 kVp and 100 kVp energies for a 5 cm diameter, 15 cm FSD applicator. These have been corrected by the response factors discussed above to depth doses in water, as measured by the diamond and parallel-plate detectors and as calculated by the Monte Carlo method described earlier; interpolated *Br. J. Radiol.* supplement 25 values are also plotted. All values plotted are normalized to the dose at 1 mm depth, as measured by the parallel-plate chamber with 100% representing the surface dose with the exclusion of contaminant electrons. Random uncertainty in the diamond and

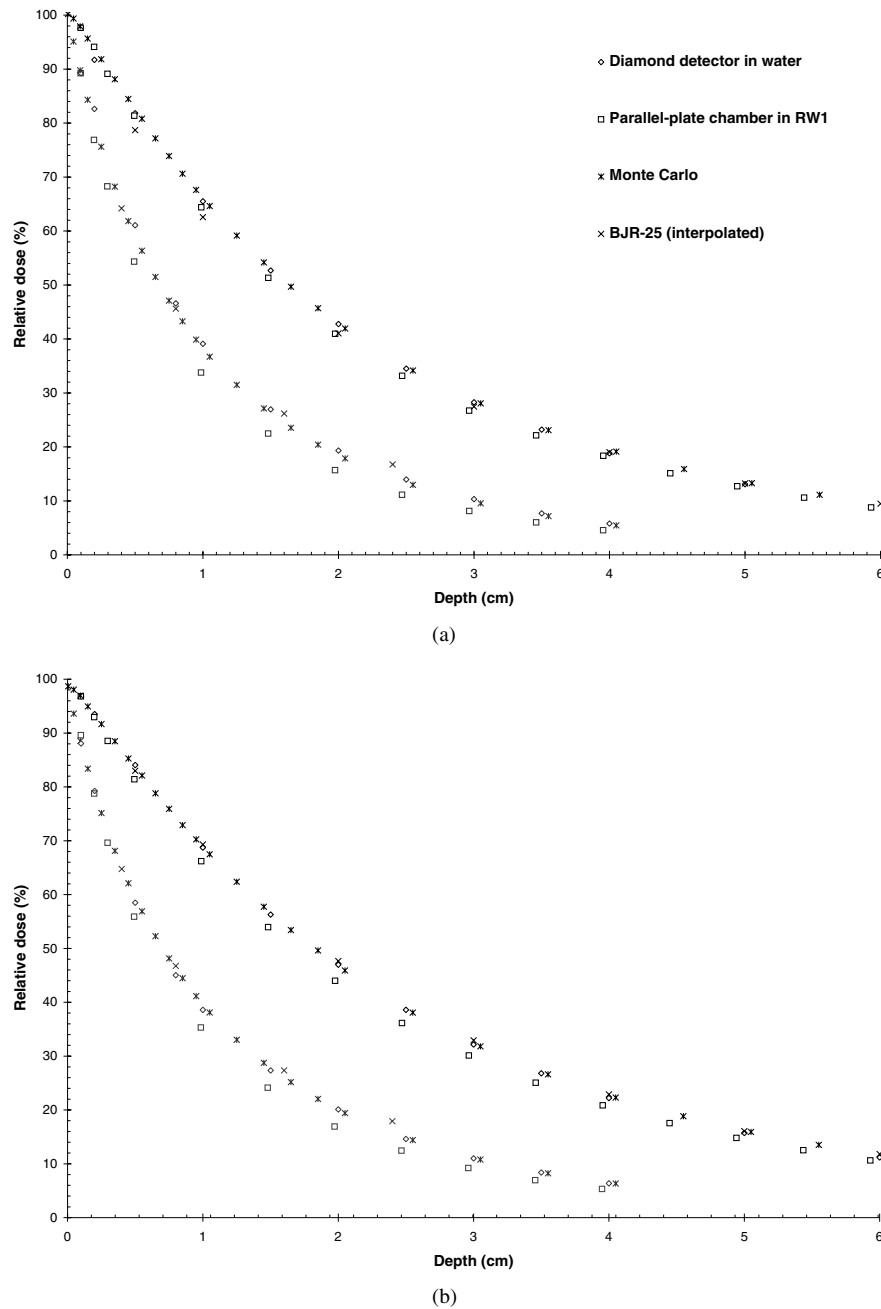


Figure 1. Percentage depth dose for and 45 kVp (0.55 mm Al HVL, lower group) and 100 kVp x-rays (2.30 mm Al HVL, upper group) for 1.5(a), 3(b) and 5 cm (c) diameter cylindrical collimators at 15 cm FSD. Readings from the diamond detector in water are normalized to the parallel-plate ionization chamber reading in RW1 material at 1 mm depth which has been normalized to 100% at the surface. The measurements are compared with calculations using the Monte Carlo method using Birch–Marshall spectra modified by data for transmission through aluminium and interpolated *Br. J. Radiol.* supplement 25 data for the matching HVL. The diamond has a dose-rate correction, the Monte Carlo model is used to correct the diamond for the mass-absorption ratio of carbon to water and the depth scaling of the parallel-plate chamber from the ratio of attenuation coefficients of RW1 to water calculated as a function of depth.

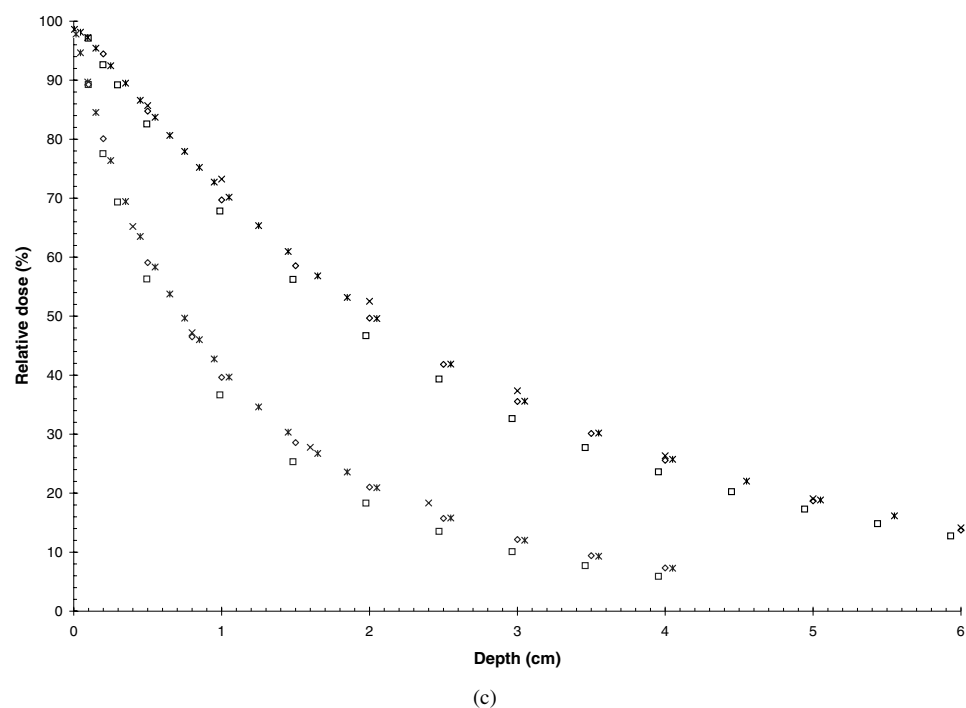


Figure 1. (Continued)

ionization chamber readings are less than 1%, while the Monte Carlo calculations are less than 0.2% (2 sd).

3.4. Relative output factors

Plots of relative output factors (normalized to the 5 cm applicator) are shown in figure 2 for both beams. These include results for the diamond detector in water, the parallel-plate chamber in RW1, as well as values derived from measured applicator factors in air, using the 0.2 cm³ Farmer cylindrical chamber and Monte Carlo derived phantom scatter factors (at a water surface). All output factors relate to measured or calculated doses at the surface of a water phantom using appropriate corrections as discussed above. The error bars represent the random uncertainty in the diamond reading; the uncertainty in the ionization chamber and prediction are of a similar magnitude given that the Monte Carlo contribution to the random uncertainty is negligible.

4. Discussion

4.1. Dose and dose-rate linearity

A linear relationship between the irradiation time and diamond detector output was clearly established over a dose range up to 8 Gy for the beams. In both cases, there existed a small negative output intercept, which is probably associated with timer uncertainties. The experimentally determined Δ values for the beams indicated minimal sublinearity in accordance with Fowler (1966). The Δ value obtained for the same diamond detector in a

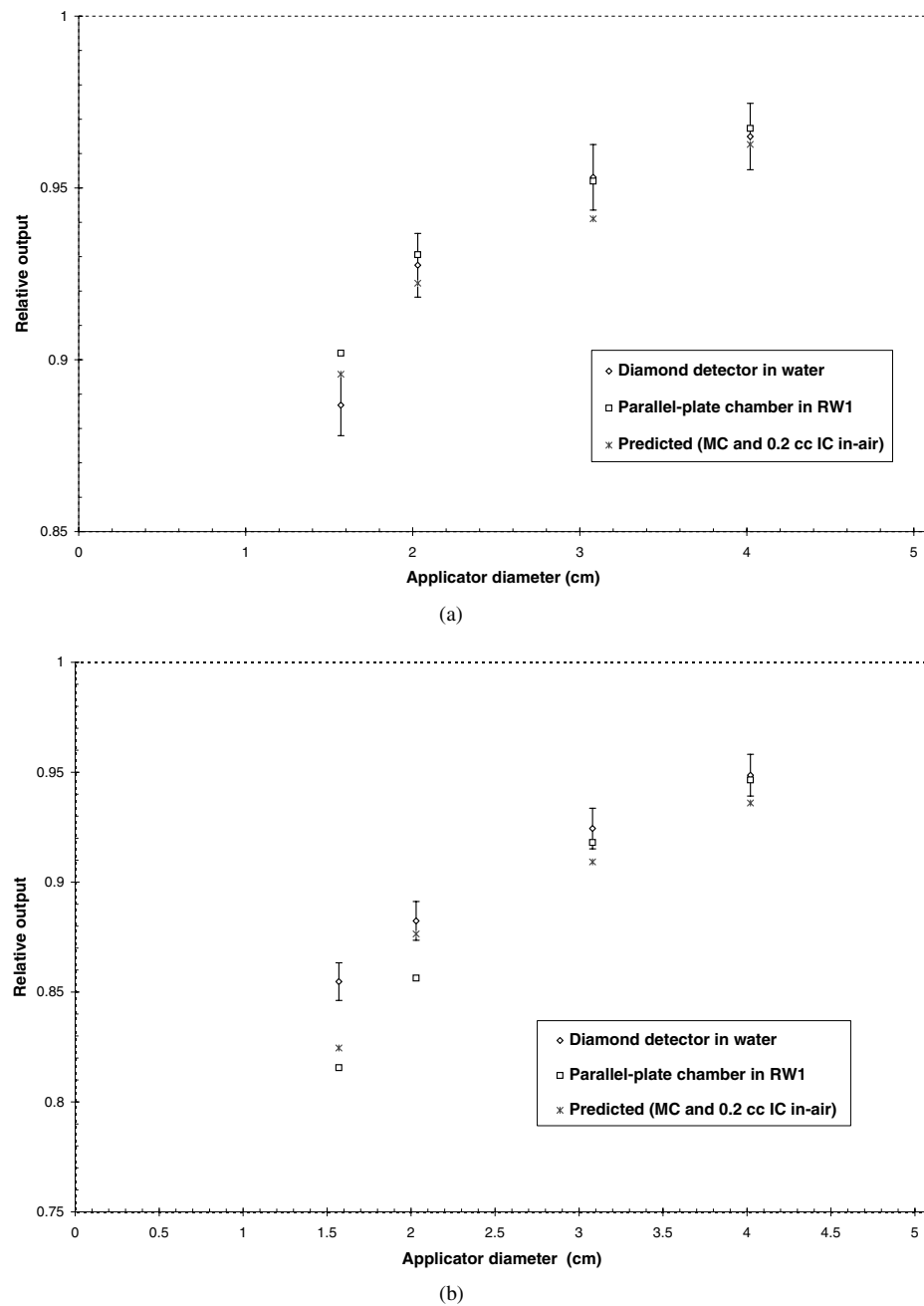


Figure 2. Output factors for 45 kVp x-rays, 0.55 mm HVL (a) and 100 kVp x-rays, 2.3 mm HVL (b) for cylindrical applicators (15 cm FSD) relative to a 5 cm diameter applicator.

5 MV beam was 0.975. The dose-rate dependence of the diamond detector has therefore been shown to be energy independent, at least in the range 50 kVp to 6 MV; it is of interest to note that Heydarian *et al* (1997) found virtually no energy dependence between 4 MV and 23 MV.

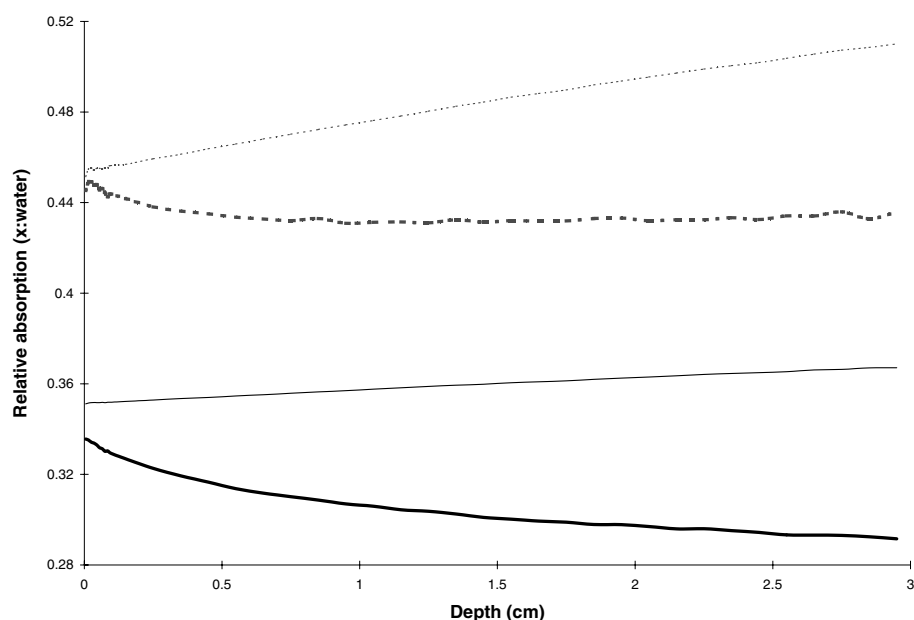


Figure 3. Theoretical Monte Carlo based models of response in polyethylene for the 45 kVp (solid) and 100 kVp (dashed) beam with the 1.5 cm applicator comparing single scatter (light), in same manner as the diamond detector, with all scatter (bold) occurring in the detector housing material.

4.2. Percentage depth doses

The excellent match between diamond detector and Monte Carlo results provides some corroboration that the modelling, including the method of obtaining the spectrum, is adequate. In this so-called Bayesian method, where the theoretical estimate of the spectra forms a prior estimate of the actual distribution, the likelihood of the estimate is maximized according to quality of the match with the experimental data and the degree of departure from the theoretical estimate. It is anticipated that higher precision is obtainable with transmission measurements using hyperpure aluminium.

The energy response has been determined for a dosimeter using a quasi-monoenergetic x-ray source by several workers. Seuntjens *et al* (1999) measured a response to compute depth in phantom quality corrections for a diamond detector, but gave an energy response for their diamonds that varies less than that of Planskoy (1980). Both measured an energy response that varied more than predicted by the mass-absorption ratio of air to carbon indicating a substantial and varying influence from the Ag/Cu contacts.

The model for correction of absorption in diamond presumes that only a single scatter occurs in the detector prior to absorption. The magnitude of the change in the mass-energy absorption ratios as a function of depth for the two beams is reasonably large, though as a proportion of the dose relative to that at the surface it amounts to a maximum discrepancy of 2.7 to 2.9% at 2 cm depth from the largest to smallest applicator in the 100 kVp beam but only 0.3% at 1 cm depth in the 45 kVp beam.

Differences between the diamond detector and parallel-plate chamber are significant, suggesting that there is perturbation of the field in the vicinity of one or both detectors. We have modelled absorption in the predominant material in each case but in the case of the parallel-plate chamber the sizeable polyethylene base is likely to perturb secondary photons at low energies.

A second model is proposed to better explain the perturbation of the photon fluence in the polyethylene base of the parallel-plate chamber. It is assumed that all interactions occur in the polyethylene wall which would correspond to small fields with the detector near the surface. Intermediate effects will occur at depth where some photons will interact in the medium for all but the last interaction with the wall, while others will interact entirely with the wall. These effects can be computed by weighting the energy of deposition events, ε_i , by a *product* of the mass-energy absorption ratios for the sequence of photon interactions.

Figure 3 demonstrates the magnitude of these effects for the 45 and 100 kVp beams with a 1.5 cm applicator. The actual perturbation factor will lie somewhere between these extreme circumstances. In particular, full scatter within the detector at the surface is expected to predominate and at depth a reasonable mixture of the two is anticipated.

4.3. Relative field outputs

The influence, particularly at the higher of the two energies, of the larger collecting volume of the parallel-plate chamber, is evident for the smallest field size. Electron disequilibrium may be also be a factor for this chamber although the electron range is no more than 0.1 mm in water at these energies. The in-air measurement of output also appears to be affected and might benefit from measurement at a larger FSD.

5. Conclusion

This paper investigates the use of diamond detectors for two superficial x-ray modalities, of peak potential 45 kVp and 100 kVp and first HVL of 0.55 mmAl and 2.3 mmAl respectively. Dose and dose-rate linearity are demonstrated. Dose versus depth and field size have been compared with a parallel-plate chamber and Monte Carlo calculations.

The Monte Carlo model provides a second function, enabling corrections for the energy dependence of the sensitive material, diamond to water, and density scaling to be included in the phantom measurements. A transmission method in combination with an analytical model is used to characterize the source. Absorption corrections have been computed concurrently using a typical form of tally.

The diamond detector demonstrates good agreement with Monte Carlo results but a systematic disagreement with the parallel-plate chamber, which we suggest is due to perturbations occurring in the polyethylene housing of the detector.

Several workers have considered explicit modelling of ionization chambers and solid state detectors in phantoms but diamond detectors and the parallel-plate chamber have yet to be examined in this energy range. Such calculations require the detector to be included in the phantom modelling, meaning that multiple simulations are required to obtain quality corrections as a function of depth and field size. We present the above methods as an alternative to detailed Monte Carlo calculations in anticipation that other centres will be able to implement this method easily. Our future work will examine perturbation factors for the parallel-plate chamber with explicit modelling of the detector housing.

References

- Birch R and Marshall M 1979 Computation of bremsstrahlung X-ray spectra and comparison with spectra measured with a Ge(Li) detector *Phys. Med. Biol.* **24** 505–17
- BJR and IPEMB Joint Working Party 1996 Central axis depth dose data for use in radiotherapy *Br. J. Radiol.* supplement 25

- Burgemeister E A 1981 Dosimetry with a diamond detector acting as a resistor *Phys. Med. Biol.* **26** 269–75
- Fowler J F 1966 Solid state electrical conductivity detectors in radiation dosimetry *Radiation Dosimetry: Instrumentation* vol 2, ed F H Attix and W C Roesch (New York: Academic) pp 291–324
- Hermann K P, Geworski L, Muth M and Harder D 1985 Polyethylene-based water-equivalent phantom material for x-ray dosimetry at tube voltages from 10 to 100 keV *Phys. Med. Biol.* **30** 1195–200
- Heydarian M, Hoban P W, Beckham W A, Borchardt I M and Beddoe A H 1993 Evaluation of a PTW diamond detector for electron beam measurements *Phys. Med. Biol.* **38** 1035–42
- Heydarian M, Hoban P W and Beddoe A H 1996 A comparison of dosimetry techniques in stereotactic radiosurgery *Phys. Med. Biol.* **41** 93–110
- Heydarian M, Zahmatkesh M, Hoban P W and Beddoe A H 1997 Dose rate correction factors for diamond detectors for megavoltage photon beams *Phys. Med.* **8** 55–60
- Hoban P W, Heydarian M, Beckham W A and Beddoe A H 1994 Dose rate dependence of a PTW diamond detector in the dosimetry of a 6 MV photon beam *Phys. Med. Biol.* **39** 1219–29
- Ipe N E, Rosser K E, Moretti C J, Manning J W and Palmer M J 2001 Air kerma calibration factors and chamber correction values for PTW soft x-ray, NACP and Roos ionization chambers at very low x-ray energies *Phys. Med. Biol.* **46** 2107–17
- Khrunov B S, Martynov S S, Vatrisky S M, Ermakov I A, Chervajakou A M and Karlin D L 1990 Diamond detectors in relative dosimetry of photon, electron and proton radiation fields *Radiat. Prot. Dosim.* **33** 155–7
- Klevenhagen S C, D'Souza D and Bonnefoux I 1991 Complications in low energy x-ray dosimetry caused by electron contamination *Phys. Med. Biol.* **36** 1111–16
- Kozlov S F, Stuck R, Hage-Ali M and Siffert P 1975 Preparation and characteristics of natural diamond detectors *IEEE Trans. Nucl. Sci.* **22** 160–70
- Namito Y, Ban S and Hirayama H 1994 Implementation of the Doppler broadening of a Compton-scattered photon in the EGS4 code *Nucl. Instrum. Methods A* **349** 489–94
- Nelson W R, Hirayama H and Rogers D W O 1985 The EGS4 code system *SLAC Report 265* (Stanford, CA: Stanford Linear Accelerator Center)
- O'Connor J E 1957 The variation of scattered X-rays with density in an irradiated body *Phys. Med. Biol.* **1** 352–69
- Ouellet R G and Schreiner L J 1991 A parametrization of the mass attenuation coefficients for elements with $Z = 1$ to $Z = 92$ in the photon energy range from ~ 1 to 150 keV *Phys. Med. Biol.* **36** 987–99
- Perrin B A, Whitehurst P, Cooper P and Hounsell A R 2001 The measurement of k_{ch} factors for application with the IPEMB very low energy dosimetry protocol *Phys. Med. Biol.* **46** 1985–95
- Plansky B 1980 Evaluation of diamond radiation detectors *Phys. Med. Biol.* **25** 519–32
- Rogers D W O 1984 Low energy electron transport with EGS *Nucl. Instrum. Methods A* **227** 535–48
- Rustgi S N 1995 Evaluation of the dosimetric characteristics of a diamond detector for photon beam measurements *Med. Phys.* **22** 567–70
- Seuntjens J, Aalbers A H L, Grimbergen T W M, Mijnheer B J, Thiereus H, Dam J V, Wittkamper F W, Zoetelief J, Piessens M and Piret P 1999 Suitability of diamond detectors to measure central axis depth kerma curves for low and medium energy x-rays *Kilovoltage X-ray Dosimetry* ed C M Ma and J Seuntjens (Madison, WI: Medical Physics Publishing) pp 227–38
- Waggener R G, Blough M M, Terry J A, Chen D, Lee N E, Zhang S and McDavid W D 1999 X-ray spectra estimation using attenuation measurements from 25 kVp to 18 MV *Med. Phys.* **26** 1269–78